Iranian Journal of Pharmaceutical Sciences
Spring 2009: 5(2): 89-94
ijps.sums.ac.ir

Original Article

Synthesis of Hydroxyapatite Nanostructure by Hydrothermal Condition for Biomedical Application

Saheb Ali Manafi*, Sedigheh Joughehdoust

Materials Engineering Department, Islamic Azad University, Shahrood Branch, Shahrood, Iran

Abstract

In this investigation, hydroxyapatite (HAp) nanostructure with uniform morphologies, controllable size, nano-dispersion and narrow-size distribution in diameter has been synthesized successfully by low-temperature hydrothermal process, and the as-synthesized powders were characterized by energy-dispersive X-ray spectroscopy, scanning electron microscopy, high-resolution transmission electron microscopy (HRTEM), Fourier transform infrared, and induced couple plasma (ICP). In the present work, a novel technique of sono-chemical of $CaHPO_4.2H_2O$/NaOH/distilled water with cetyltrimethylammonium bromide ($(CH_3(CH_2)_{15}N^+(CH_3)_3Br^-$) designated as CTAB) under hydrothermal condition to synthesize HAp nanostructure was described. Furthermore, the usage of a high basic condition a water environment is the two crucial keys in ensuring the formation of HAp the hydrothermal/sonochemical processes. However, the crystallite size and crystallinity degree of the HAp increased with the addition of annealing temperature. Indeed, the present work will introduce new method in synthesis of HAs for scientific and medical engineering.

Keywords: Biocompatibility; Hydrothermal condition; Hydroxyapatite; Nanocrystalline; Tissue engineering.
Received: December 4, 2007; *Accepted:* November 20, 2008

1. Introduction

There is an escalating interest in calcium phosphates, particularly apatites, which seems to be driven mainly by the requirements for the development, understanding, and manufacture of biomaterials [1]. Compounds with the apatite ($Ca_{10}(PO_4)_6(F, Cl, OH)_2$) structure have been widely studied due to their potential applications as biomaterials [2], catalysts [3], ion exchangers [4], oxide ion conductors [5], and luminescent materials [6]. Many synthetic strategies have been developed to produce these nanostructures, such as the solid-state reactions [7] and sol-gel method [8]. Recently, hydrothermal reactions have been used successfully as a non-traditional way of producing nanopowder, single crystals, and nanostructure [9-11]. Depending on the supersaturation level and the solution pH, a number of calcium phosphates may be formed at ambient temperatures and pressure. In aquatic solution of pH>4, the order of increasing solubility is as follows: tricalcium phosphate

*Corresponding author: Saheb Ali Manafi, Materials Engineering Department, Islamic Azad University, Shahrood Branch, Shahrood, Iran, P.O. Box 36155-163.
Tel (+98)273-3334530, Fax (+98)273-3334537
E-mail: ali_manafi2005@yahoo.com

($Ca_3(PO_4)_2$, TCP), octa-calcium phosphate ($Ca_4H(PO_4)_3.2.5H_2O$, OCP), dicalcium phosphate dihydrate ($CaHPO_4.2H_2O$, DCPD), and hydroxyapatite (HAp) with a hexagonal structure with space group $P6_3/m$ and lattice parameters a=b=9.4225 Å and c=6.8850 Å [12]. There are two formula units per unit cell and the arrangement is typical of the calcium apatites and can be viewed as consisting of unconnected, robust PO_4^{-3} tetrahedral with Ca^{+2} in the space between and a chain of OH^- ions along the c-axis to balance the change (Figure 1). Monoclinic structures with four formula units permit unit cell have also been reported [13, 14], where the monoclinic unit cell is obtained from the hexagonal one by doubling the b lattice parameter and by having different arrangements of the anion chains. Difficulties in obtaining the stoichiometric compound, particularly with regarded to the hexagonal phase of HAp presents a problem. Following failed attempts to fix X-ray diffraction data using the space group $P6_3$, the structure was found with space group $P6_3/m$ through the addition of two mirror planes perpendicular to the (001) and passing through z=1/4 and z=3/4. However, this structure has four possible sites for the two OH groups per unit cell, a difficulty which was resolved by assuming 0.5 occupancy per site resulting from disorder in very anion column or disorder from column to column [15]. Among of them, HAp, thermodynamically the most stable calcium phosphate salt, has been extensively studied because it is the main inorganic compound of hard tissues in vertebrates. Although the precipitation of HAp is of particular importance in the biomineralization processes, very little is known about the crystal growth mechanism. In present work, the hydrothermal technique was developed for the formation of HAp nanostructures. The nano-HAp is interestingly crystalline with high-yield. These high-quality HAp nanorods represent well-defined nanoscale structure needed for both fundamental studies and clinical applications.

2. Materials and methods

In the present work, the alkali solution of HAp was prepared by dissolving $CaHPO_4.2H_2O$/NaOH/distilled water, followed by adding 2.0-3.0 g cetyltrimethylammonium bromide (CTAB). Before being transferred to a Teflon-lined autoclave, the solution mixture was pretreated under an ultrasonic water bath for 30-40 min. The hydrothermal syntheses were conducted at 150 °C for 2 h in an electric oven. After the reactions, white paste products (HAp nanorods) were harvested by and decanted

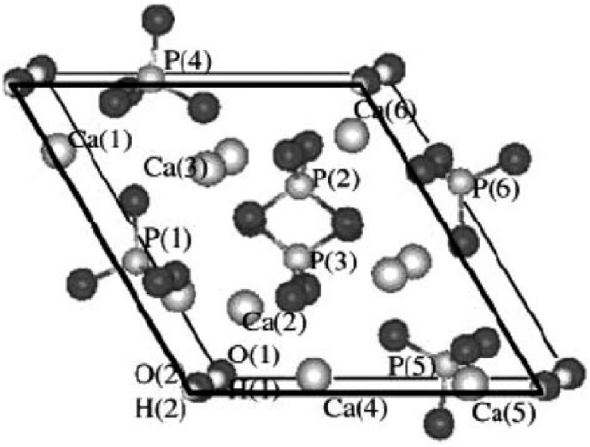

Figure 1. Hydroxyapatite structure viewed along the c axis.

with distilled. The obtained HAp nanorods were characterized with scanning electron microscopy, energy-dispersive X-ray spectroscopy (SEM/EDX, XL30), and transmission electron microscopy. The size distribution and morphology of the samples were analyzed by field emission gun (FEG) transmission electron microscope, selected area electron diffraction (TEM/SAED observation on a Philips CM200 transmission electron microscope operated at 200 kV). X-ray diffraction (XRD) patterns were recorded in the angular range 2θ=20-60º. For these experiments, a Siemens diffractometer (30 kV and 25 mA) with the $K_{\alpha 1}$, radiation of copper (λ=1.5406 Å), was used. The powder product was further investigated using Fourier transform infrared (FT-IR) spectroscopy in a Bruker-IR spectrometer from 500 to 4000 cm^{-1} using the KBr technique and operating in the transmittance mode.

3. Results and discussion

In Figure 2, the XRD patterns of the three samples are presented. It can be found that, with the prolonging of the reaction time, the basal lines of the samples become flattened, which indicates that the crystalline quality of the samples improved. Furthermore, the intensity of the peaks of HAp also increased when the reaction time prolonged in constant temperature 150 °C. This result may indicate that, amorphous HAp transformed into crystalline HAp under high-temperature and high-pressure hydrothermal conditions. Moreover, at a higher temperature of 200 °C, the peak ascribed to HAp phases show better crystallization compared with HAp formed 150 °C even for a long reaction time. It means that the rates of precipitation and the crystallization increase with the temperature and the reaction period, resulting in lager size and that cause sharper peaks of XRD. So, we may conclude that the HAp powders do not crystalline completely below 150 °C (not shown).

Figure 3 shows the SEM image of HAp nanostructures. The typical spherical HAp nanostructures consisted of the HAp rod-like with 50-30 nm in diameter and several micrometers in length. By definition of the rod-like HAp nanostructures, it is impossible that the aggregation resulted in the rod-like nanostructures, because long time ultrasonic treatment could not destroy the nanostructures.

In Figure 4, TEM image reveals the morphology of nanostructure formed at 150 °C for 20 h with diameters of 15-40 nm and length of 70-150 nm. It is quite obvious that the morphologies of the products change considerably as a functions of the residence

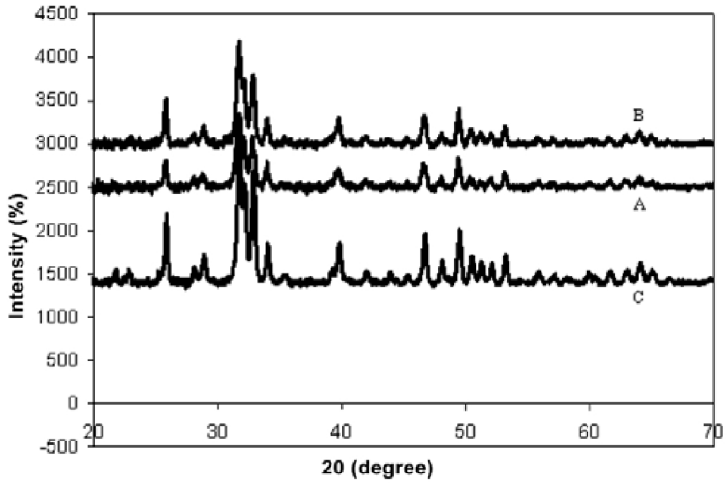

Figure 2. XRD patterns of HAp samples at different reaction times. (A): 15 h, (B): 20 h and (C): 25 h.

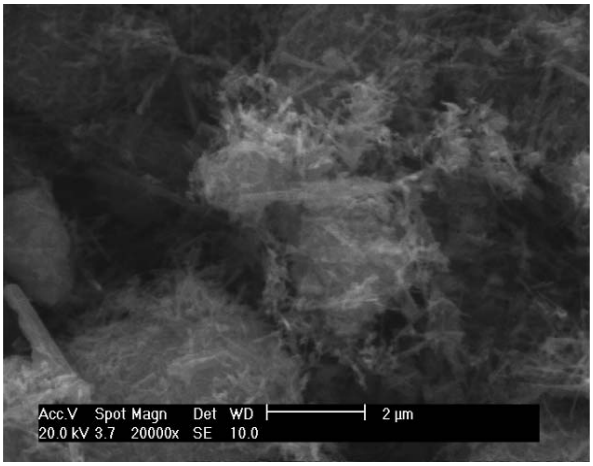

Figure 3. SEM images of as-synthesized HAp obtained at hydrothermal condition.

time in the autoclave. On the basis of the morphologies observed by TEM, it can be concluded that the size of the particles increase with the increase of reaction time, a fact that is consistent with the results of the XRD patterns.

The selected area electron diffraction (SAED) pattern taken from the as-prepared HAp nanostructure synthesized at 150 °C for 20 h consists of a number of rectangular and some distinct spots along the ring contours, suggesting a hexagonal structure. The spots in an electron diffraction pattern arise due to the diffracted electron beam from a set of lattice planes in the crystalline present in the sample satisfying the Bragg diffraction condition. In other words, the ring is an envelope of all diffracted spot. Among same of the rings a few spots appear to be prominent, which indicates the formation of crystallites. The interplanar spacing values are calculated from Bragg's diffraction equation using the diffraction ring diameter and the camera length of the TEM. The chemical stoichiometry of nanorods was investigated with EDX which indeed gave an atomic ratio of HAp ~ 1.67. At the same time, this result is consistent with the

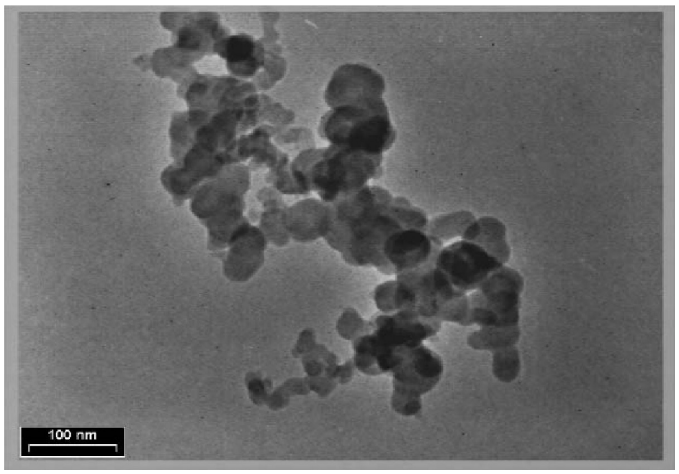

Figure 4. TEM images of HAp nanostructure.

inductively coupled plasma (ICP) calculation. More details about the structure of HAp nanostructures were investigated by the SAED pattern and TEM.

FT-IR analysis revealed the presence of carbonate on the surface of the HAp. FT-IR showed the transmittance infrared spectrum of synthetic HAp in the 4000-650 cm^{-1} region. A narrow band located near 965 cm^{-1} represents the υ_1 mode of PO_4^{3-} ions in apatite. The main signal of phosphate appears in the triply degenerate υ_3 domain (1000-1100 cm^{-1}). The adsorption band at 3500 cm^{-1} confirmed the presence of OH^- groups. The υ_2 peak of CO_3^{2-} is located at 875 cm^{-1}; this absorption results from out-of plane stretching. The υ_3 mode, near 1400 cm-1, is the strongest IR peak for carbonate. This peak is actually composed of two bands [16, 17]. The shape of the υ_3 signal and the absence of the C-O absorption bands at 700 cm^{-1} indicate that no calcite was associated with the HAp. Carbonate ions can substitute for either OH^- or PO_4^{3-} ions in the apatite structure (type A CO_3^{2-} or type B CO_3^{2-}) [18, 19].

4. Conclusion

In summary, an effective method was developed for the formation of ultra-crystallinity rod-like HAp. The nano-rods are highly high aspect-ratio, high-crystalline and uniformly structured. These high-quality HAp nano-rods represent well-defined nanoscale structure needed for both fundamental studies and clinical applications. As the matter of fact, this method (hydrothermal synthesis) guarantees its production in the synthesis of HAs for different applications.

5. Acknowledgments

The authors thank the Tarbiat Modarres University for access to SEM and technical support. So, the authors would like to acknowledge Mr. Nouri for helping in preparing of this paper and Mr. Jabbari for performing the experimental tests.

References

[1] Elliott JC. Recent studies of apatites and other calcium orthophospates. In: Bres E, Hardouin P, (editors). *Calcium Phosphate Materials, Fundamentals*. Monpellier: Sauramps Medical, 1998; p. 25.

[2] Suchanek W, Yoshimura M. Processing and properties of hydroxyapatite-based biomaterials for use as hard tissue replacement implants. *J Mater Res* 1998; 13: 94-117.

[3] Monma H. Catalytic behavior of calcium phosphates for decomposition of 2-propanol and ethanol. *J Catal* 1982; 75: 200-3.

[4] Sugiyama S, Matsumoto H, Hayashi H, Moffat JB. Sorption and ion-exchange properties of barium hydroxyapatite with divalent cations. *Colloid Surface A* 2000; 169: 17-26.

[5] Slater PR, Sansom JE, Tolchard JR. Development of apatite-type oxide ion conductors. *Chem Rec* 2004; 4: 373-84.

[6] Blasse G. The physics of new luminescent materials. *Mater Chem Phys* 1987; 16: 201-34.

[7] Nakayama S, Sakamoto MJ. Electrical properties of new type high oxide ionic electrical properties of new type high oxide ionic conductor $RE_{10}Si_6O_{27}$ (RE=La, Pr, Nd, Sm, Gd, Dy). *Eur Ceram Soc* 1998; 18: 1413-8.

[8] Tao S, Irvine JTS. Preparation and characterisation of apatite-type lanthanum silicates by sol-gel processes. *Mater Res Bull* 2001; 36: 1245-58.

[9] Andres-Verges M, Fernandez-Gonzalez C, Martinez-Gallega M. Hydrothermal synthesis of calcium deficient hydroxyapatites with controlled size and homogeneous morphology. *J Eur Ceram Soc* 1998; 18: 1245-50.

[10] Nagata F, Yokogawa Y, Toriyama M, Kawamoto Y, Suzuki T, Nishizawa K. Hydrothermal synthesis of hydroxyapatite crystals in the presence of methanol. *J Ceram Soc Jpn* 1995; 103: 70-3.

[11] Kumar R, Prakash KH, Cheang P, Khor KA. Temperature driven morphological changes of chemically precipitated hydroxyapatite nanoparticles. *Langmuir* 2004; 20: 5196-200.

[12] Elliott JC. *Structure and chemistry of the apatites and other calcium orthophosphates*. Amsterdam: Elsevier, 1994.

[13] Morgan H, Wilson RM, Elliott JC, Dowker SEP, Anderson P. Preparation and characterisation of monoclinic hydroxyapatite and its precipitated carbonate apatite intermediate. *Biomaterials* 2000; 21: 617-27.

[14] Haverty D, Tofail SAM, Stanton KT, McMonagle JB. The structure and stability of hydroxyapatite.

Phys Rev B 2005; 71: 94103-9.
[15] Kay MI, Young RA. Crystal structure of hydroxyapatite. *Nature* 1964; 204: 1050-2.
[16] Doi Y, Moriwaki Y, Aoba T, Takahashi J, Joshin K. ESR and IR studies of carbonate-containing hydroxyapatites. *Calcif Tissue Int* 1982; 34: 178-81.
[17] Reigner P, Lasaga AC, Berner RA, Han OH, Zilm KW. Mechanism of CO (Super 2-) 3 substitution in carbonate-fluorapatite; evidence from FTIR spectroscopy. *Am Mineral* 1994; 79: 809-18.
[18] Elliot JC. The crystallographic structure of dental enamel and related apatites. Ph.D Thesis, London: University of London, 1964.
[19] Bonel GA. Contribution an l'etude de la carbonation Des apatites. *Ann Chim* 1972; 7: 65-87.